Laser cooling, trapping and spectroscopy of calcium isotopes

Mollema, Albert Kornelis

Chapter 4

Light pressure induced spectroscopy

This chapter is based on A. K. Mollema, L. W. Wansbeek, L. Willmann, K. Jungmann, R. G. E. Timmermans, and R. Hoekstra, Phys. Rev. A **77**, 043409 (2008). *Monte Carlo simulations were performed by L. W. Wansbeek.*

4.1 Introduction

In numerous experiments involving for example laser cooling and trapping, precision spectroscopy, metrology, atom trap trace analysis or resonant-ionization mass spectrometry it is of key importance that the laser is frequency referenced and/or stabilized. Over the years a whole arsenal of spectroscopy methods [63] has been developed to meet the needs in the different areas of application. Nonlinear spectroscopy techniques such as saturation and polarization spectroscopy are widely used. In these methods a strong pump laser beam is used to change state populations, which in turn affect the absorption of a weak counter-propagating probe laser beam. The shapes of the spectroscopy signals [74–76] are slightly distorted by the photon momentum transferred to the atoms in the gas which leads to a redistribution of the atomic velocities. On a larger scale this light force is used to slow down, deflect, or trap atoms (see e.g. Ref. [40]).

In this chapter we demonstrate a beam-based spectroscopy technique that exploits the light-pressure-induced redistribution of the transverse atomic velocities to obtain a dispersive signal that can directly be used for frequency stabilization purposes. The basic idea behind this **Li**ght-**P**ressure induced **S**pectroscopy (LiPS) is the following: A relatively strong pump beam and a weak probe beam, both having the same frequency, are sent anti-parallel through an atomic beam. The probe beam does not overlap with the pump beam, but intersects the atomic beam downstream from the pump beam. The pump beam induces a distortion on the transverse velocity distribution of the atomic

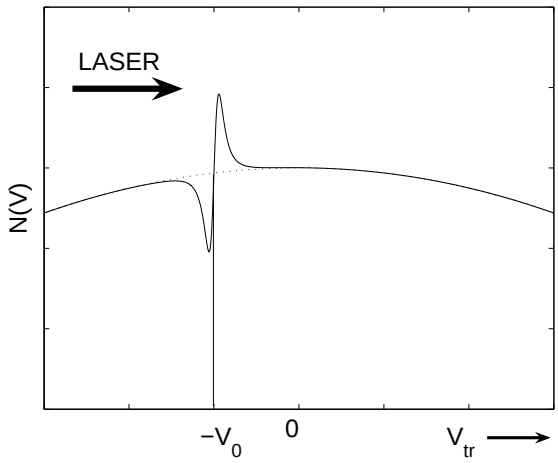

Figure 4.1: *Schematic representation of the redistribution of the transverse velocities in an atomic beam as induced by a red-detuned laser beam coming from the $-v_{tr}$ direction.*

beam. This is illustrated schematically in Fig. 4.1 for a red-detuned laser coming from the $-v_{tr}$ direction. Because of the Doppler shift the laser light is in resonance with atoms having a transverse velocity of $\sim -v_0$.

Downstream of the pump beam the probe beam samples the modified transverse velocity distribution. Since the probe beam has exactly the same frequency as the pump beam and crosses the atomic beam in the opposite direction, it will only experience the induced transverse velocity changes when the laser is in (near-)resonance with the unshifted atomic transition, i.e. both beams interact with atoms with transverse velocities at or close to zero. For example, for the case shown in Fig. 4.1 the probe will interact with atoms of velocities near v_0, an unaltered part of the velocity distribution, and therefore, with or without pump the absorption of the probe light is the same. Only when $v_0 \simeq 0$ the absorption of the probe beam is modified by the presence of the pump beam.

It will be shown that the difference in absorption of the probe beam with or without the pump beam yields a dispersive-like signal, of which the zero-crossing is only slightly red-detuned from the atomic transition frequency. In addition to yielding a strong dispersive signal the method has as an advantage that it may be applied to atomic systems for which it is hard to produce vapor cells. Moreover the method is experimentally simple: in contrast to traditional saturation absorbtion techniques no frequency modulation or polarization optics is needed to obtain the dispersive-like signal.

In the following, the experimental lay-out of the LiPS technique will be presented and the method will be applied to the case of Ca atoms. The simple electronic structure of the even Ca isotopes simplifies Monte-Carlo simulations of the LiPS signals. The determination of the position of the zero-crossing in the signal by means of the Monte-

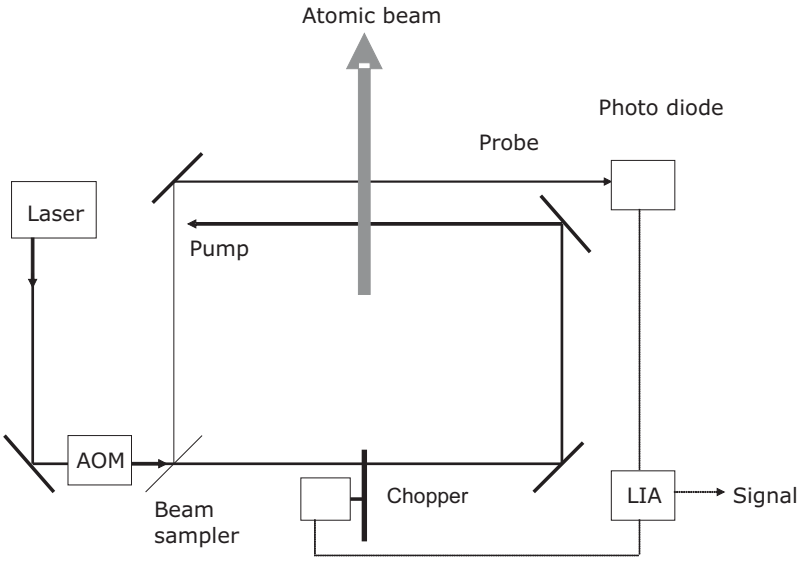

Figure 4.2: *Schematics of the LiPS setup. The AOM is double passed and is used to scan the frequency of the laser light used for LiPS. The quality of the spectroscopy signals is enhanced by using lock-in amplification.*

Carlo simulations is verified experimentally by comparison to Doppler-free saturation spectroscopy and laser-induced fluorescence.

4.2 LiPS: experimental layout and results

Experimental setup

The spectroscopy experiments were performed on the atomic beams of Ca atoms evaporated in oven 2, see Chapter 3 and [11, 21]. The $4s^2\ ^1S_0$ - $4s4p\ ^1P_1$ resonance transition in ^{40}Ca has a wavelength of 422.79 nm. This transition has a natural linewidth $\Gamma = \gamma/2\pi = 34.63$ MHz. The on-resonance saturation intensity $I_s = 59.9$ mW cm^{-2} [40].

A schematic representation of the setup used for LiPS is shown in Fig. 4.2. The oven was heated to 570 °C to provide the atomic beam. The vacuum base pressure is maintained in the lower 10^{-8} mbar range with a 30 l/s ion-getter pump (cf Chapter 3). About 10 cm down stream of the oven the LiPS measurements are performed. The pump and probe laser beams enter and exit the vacuum chamber through AR-coated viewports. For the measurements described here the pump and probe beams were separated by 3 mm along the laser beam axis. The laser beams cross the atomic beam in opposite directions. The absorption signal was recorded using a photodiode (Thorlabs DET36A/M). To enhance the quality of the signals, a lock-in amplification

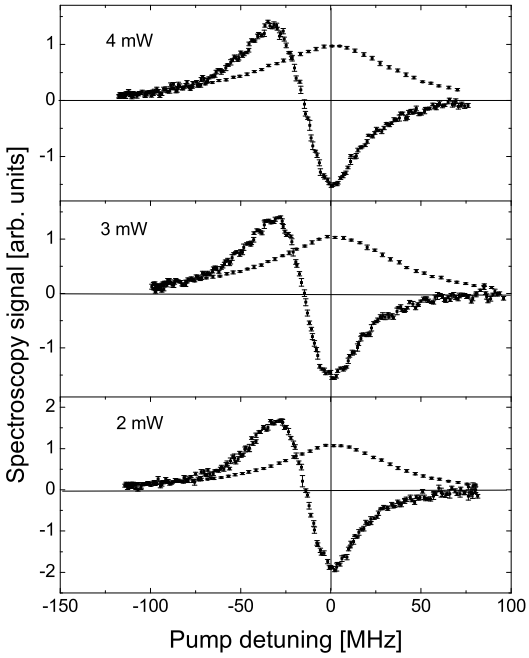

Figure 4.3: *LiPS (dispersivelike) and saturation absorption (single peak) spectra taken at different pump powers. For each individual panel, the zero of the frequency scale is taken to be defined by the maximum in the saturation absorption spectrum. The intensity scale is arbitrary but the same in all the panels.*

detection scheme was employed for which the pump beam was amplitude modulated with a mechanical chopper (Scitec Instruments 300C at 3 KHz) and a lock-in amplifier (LIA) was used (FEMTO LIA-MV-150-S).

The laser frequency was scanned with an Acousto-Optical Modulator (AOM) (Brimrose TEF-200-100-423) with a center-frequency of 200 MHz in double pass configuration. The AOM was controlled by a VCO (voltage controlled oscillator) based AOM-driver unit (Isomet D325). The dependence of the diffraction efficiency of AOM crystals on the frequency of the applied RF-signal was compensated by a feedback scheme which kept the output power constant over the whole scanning range of the AOM. A function generator provided the AOM-driver with a triangle shaped VCO-input signal (0 to 10 V) at approximately 0.1 Hz. The intensity of the probe beam is about 5% of the pump beam.

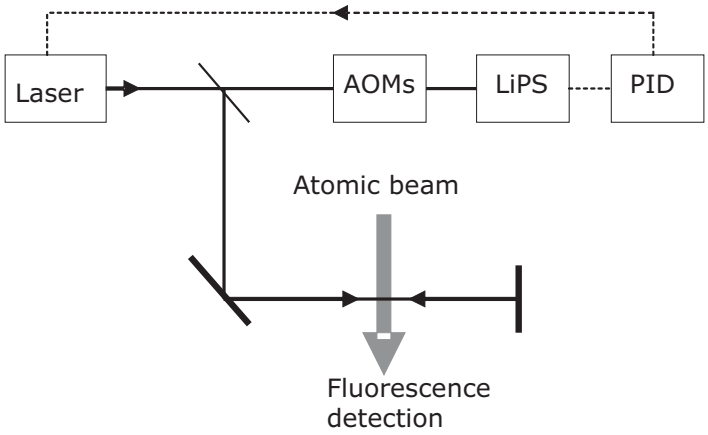

Figure 4.4: *A schematic overview of the LIF setup used to determine the zero-crossing of the LiPS signal. The laser-induced resonance fluorescence is detected using a PMT positioned normal to the plane defined by the atomic and the probe beam. The PID-controller is used to frequency-stabilize the laser onto the LiPS zero-crossing as a reference. See the text for more details.*

Spectroscopy results

In Fig. 4.3 the LiPS spectra obtained with three different pump powers (2, 3 and 4 mW) are presented. From Fig. 4.3 it can be seen that neither the width, nor the zero-crossing, nor the strength of the LiPS signal depend significantly on the pump power.

It appears that for each LiPS spectrum the zero-crossing is red-detuned by several tenths up to one half of a line width ($\Gamma = 34.63$ MHz). However, in each individual panel the maximum of the saturation absorbtion signal is taken as the atomic resonance frequency. As pointed out before [74–79], due to the modification in the transverse velocity distribution of the atoms caused by the pump beam, the position of the maximum of the saturation absorption peak is blue shifted with respect to the transition. The LiPS and saturation absorption spectroscopy signals were obtained simultaneously by splitting off a second probe beam of the initial laser beam. This second probe was overlaid with the pump beam. The counterpropagating pump and probe were aligned such that they made a small angle ($\sim 2°$) with respect to each other. The overlap angle and the uncertainties therein are another source of uncertainty for the saturation absorbtion spectroscopy signals. The absolute calibration of the saturation spectroscopy spectra will be discussed in more detail in the next sections.

As a second independent approach to determine the zero-crossing of the LiPS signal laser-induced fluorescence (LIF) spectroscopy [63] was performed. The experimental lay-out of the LIF setup is depicted in Fig. 4.4. In order to do so, we stabilized the laser using the LiPS signal as a reference. By shifting the frequency of the light used for LiPS with two AOMs, one of them in double pass configuration, it was possible to

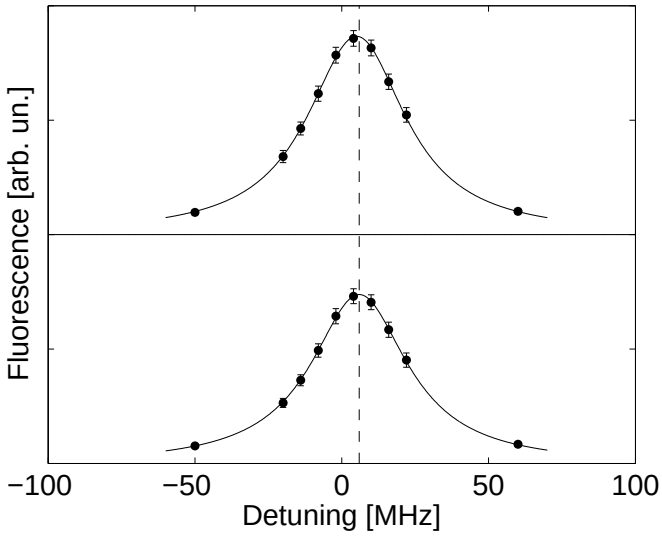

Figure 4.5: *Example of a LIF data set. 0 on the frequency axis indicates where LiPS stabilizes the laser. Upper panel: double-passed LIF probe. Lower panel: single pass LIF probe. The dashed vertical line indicates the peak position obtained from the fit of the single pass data.*

stabilize the laser in a range of some 120 MHz around the resonance transition in ^{40}Ca. Approximately 1 m downstream from the LiPS setup the atomic beam was intersected by another probe beam and the fluorescence was measured. To avoid any influence of the LiPS pump beam on the fluorescence measurement, the laser beam for the LIF experiments intersects the atomic beam perpendicular to the plane in which LiPS is performed. By measuring the fluorescence at frequencies around the resonance transition we were able to determine at which detuning the LIF signal maximizes and so to determine the detuning at which the LiPS signal crosses zero. An example spectrum is given in Fig. 4.5. To avoid an artificial shift due to a small deviation from the optimal 90° angle between atomic and probe beam, both single- and double-pass experiments were performed. In the double-pass experiments the probe has been retro-reflected onto itself. From the shift between the apparent peak positions in the single and double-pass measurements the angular deviation can be calculated [39]. In this way the angle between laser and atomic beam was optimized to 90°. The single pass data was fitted with a lorentzian function L_s. The reflected data was fitted with a sum of two lorentzians: $L_t = L_s + L_r$ in which the parameters obtained from the single pass fit were fixed. The only variables in this fit were the parameters of L_r. The location of the 0-crossing is assumed to be exactly in between the peak position of L_s and L_r.

From the fact that the shift in peak position of the single pass and double pass spectra as presented in Fig. 4.5 is only ~ 2 MHz, we can conclude that the angle of the

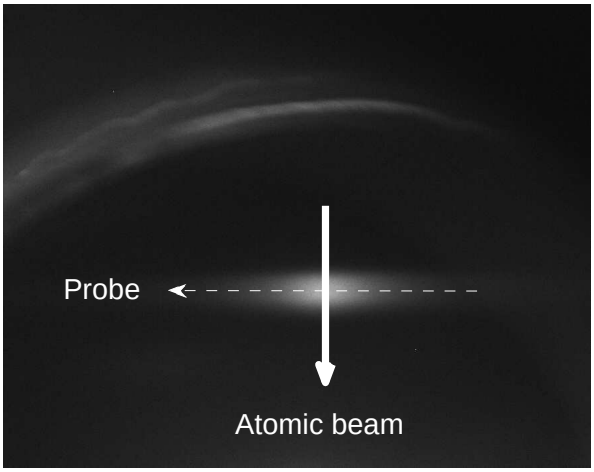

(a)

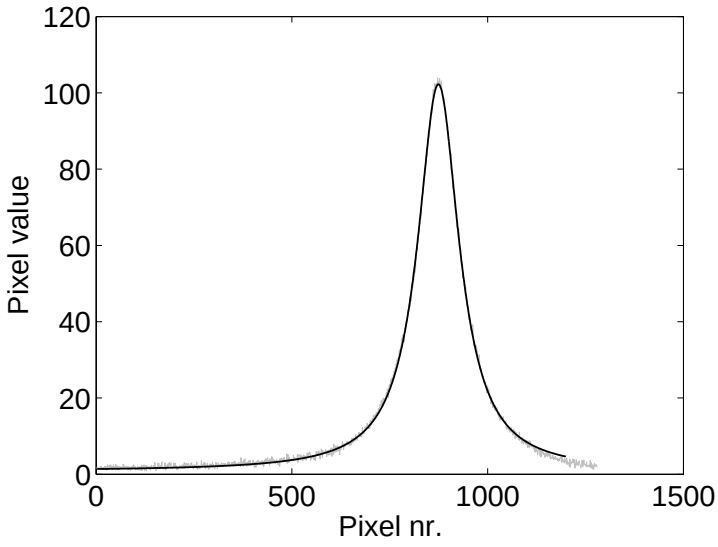

(b)

Figure 4.6: *(a) CCD image of the fluorescence induced by the weak probe beam. (b) Cross section of the CCD image fitted with a Lorentzian line shape. From this fit the peak position on the CCD chip can be determined.*

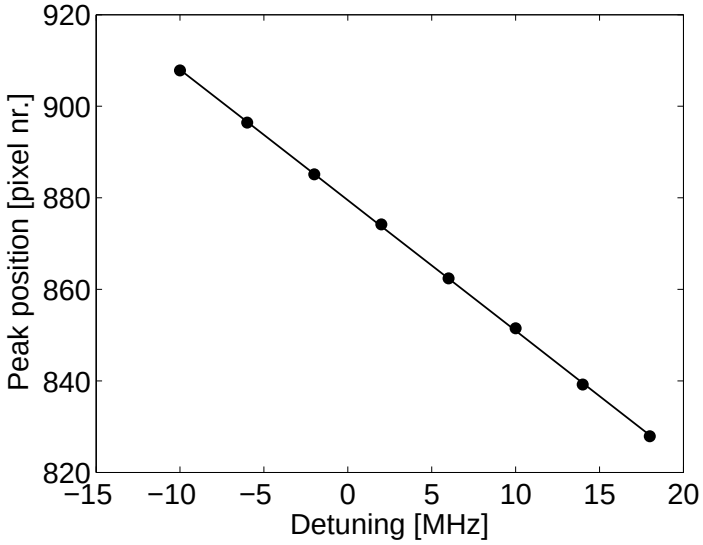

Figure 4.7: *Peak position on the chip as function of probe detuning fitted by a straight line.*

LIF probe with the atomic beam is very close to 90°

For the LIF experiments the saturation parameter s_0 of the probe beam was 0.5. In the approximation that the detuning $\delta = 0$ the scattering rate Γ_p is given by (cf. Eq. 2.15)

$$\Gamma_p(s_0) = \Gamma \frac{s_0/2}{1+s_0}. \tag{4.1}$$

When the probe is reflected onto itself, the intensity at the point in the atomic beam from where the fluorescence is collected doubles to $s_0 = 1$. The expected ratio in peak height between the reflected and single pass measurement is therefore $\Gamma_p(1)/\Gamma_p(0.5) \approx 1.5$. A ratio of ~ 1.2 was actually measured. The 20% difference is probably due to losses on the reflecting mirror and the vacuum window which had to be passed twice by the beam.

Long term stability of the LiPS signal

To check long-term stability of the dispersive-like LiPS signal, we used it to frequency stabilize the laser. A PID (proportional-integral-derivative) controller was used to lock the laser to the zero-crossing (cf. Chapter 3). To test the frequency fluctuation the following experiment was performed. A weak, tunable probe beam was sent through

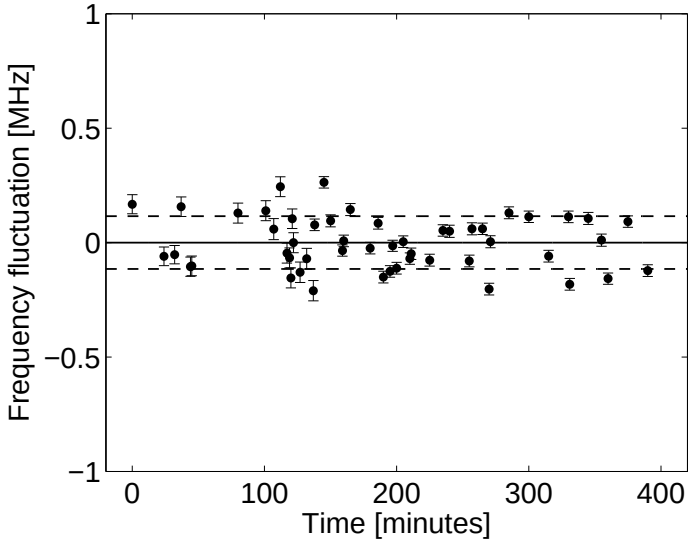

Figure 4.8: *Measurement of the fluctuations of the laser frequency when the laser is stabilized using LiPS. Error bars on the data points indicate the uncertainty of the Lorentzian fit (see text for details). Dashed lines indicate one standard deviation of the data average.*

the atomic beam. This beam was aligned parallel with the LiPS laser beams, but sent through the atomic beam just below the plane in which LiPS was performed, to exclude any disturbance on the LiPS signal. If the weak probe beam has the same frequency as the LiPS beams, it is in resonance with the atoms. This results in a fluorescence distribution in the atomic beam which can be measured using a CCD camera, see Fig. 4.6(a). The fluorescence profile was fitted with a Lorentzian line shape from which the location of the peak on the CCD camera could be determined (Fig. 4.6(b)).

When the frequency of the laser shifts, the peak position shifts as well. By taking CCD images of the weak probe beam fluorescence, the frequency fluctuation in time can be monitored. The peak position was calibrated by a scan over 25 MHz of the weak probe beam, see Fig. 4.7.

The results of a typical series of frequency fluctuation measurements are shown in Fig. 4.8. It turned out that over a period of 400 minutes, the standard deviation of the data was 0.12 MHz, which is 0.35 % of the natural linewidth Γ. This is more than sufficient for laser cooling and trapping experiments, and comparable to results obtained by other methods (cf. eg. [80–82]).

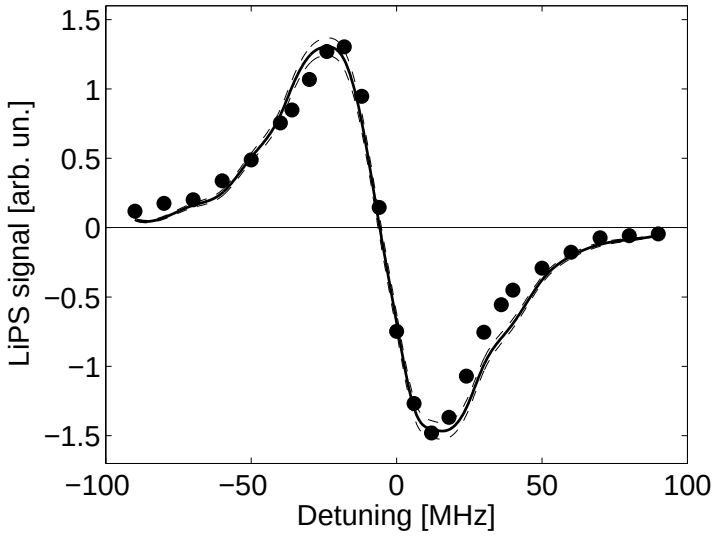

Figure 4.9: *Comparison of the experimental (●) and simulated LiPS signals as a function of the detuning of the laser frequency. The dashed line indicates the statistical uncertainty of the simulation. The laser power of the pump beam was 3 mW ($s_0 = 2.5$). The experimental data (taken from Fig. 4.3) have been frequency shifted to make the zero-crossings match. See text for more details.*

4.3 LiPS: Monte-Carlo simulation

We have performed Monte-Carlo (MC) simulations to generate LiPS signals for comparison to the experimental data. First, the effect of the pump laser on the transverse velocity distribution of the atomic beam is simulated. Thereafter, the absorption of the probe laser and its difference to the case without pump beam is calculated. The difference in absorption as a function of laser frequency,

$$\Delta(\nu, P) = A(\nu, P) - A(\nu, 0),$$

where $A(\nu, P)$ is the absorption of the probe beam at a frequency ν and a power P of the pump beam, can then be compared to the experimental LiPS signals. Due to the small radius ($\sim$ 0.8 mm) of the pump beam, the $4s^2\ ^1S_0$ - $4s4p\ ^1P_1$ resonance transition in ^{40}Ca already saturates at low laser powers. This makes analytical calculations difficult, and we resort to the relative ease and flexibility of a MC simulation.

We simulate the paths of the atoms through the two lasers by assigning an initial velocity vector (v_x, v_y, v_z) to each atom. These velocities are drawn randomly from three distributions. For the longitudinal z-direction we took a Maxwell-Boltzmann

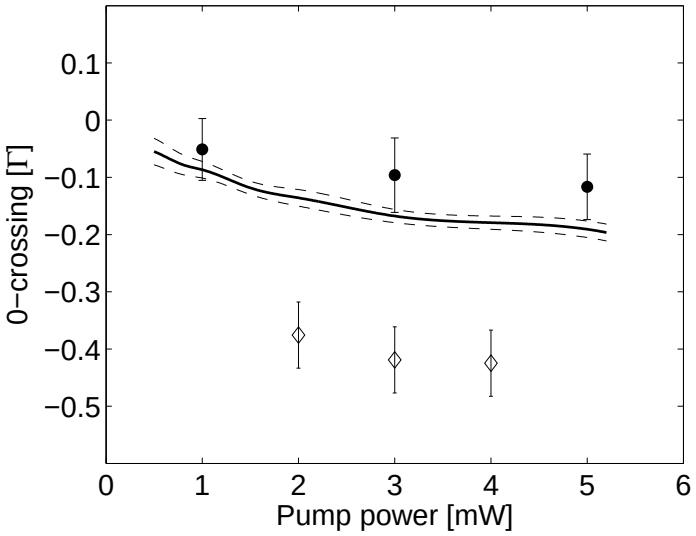

Figure 4.10: *Position of the LiPS zero-crossing in units of natural linewidth at different pump powers: ●: laser induced fluorescence, ◇: assuming Doppler-free saturation spectroscopy as a reference for the atomic transition, and −: Monte-Carlo simulation. The dashed lines indicate the statistical uncertainty of the simulation.*

distribution, with the oven temperature T and the mass of the atom m as parameters. This is very similar to the distribution suggested by Pauly [83]. For the transverse velocities we took normal distributions $N(0,\sigma^2)$, with mean 0 and a width of $\sigma = 8$ m/s. This is a good approximation to the distribution calculated by Greenland et al. [84] for pinhole atomic sources. The atom is then allowed to interact with the pump laser.

The program runs with a discrete time-step Δt. At each time-step, the time it would take the atom to absorb a photon is generated from

$$t_a = -\log(R)/W,$$

where R is a random number uniformly distributed on $[0,1]$ and

$$W = \frac{s_0\gamma/2}{1+\left(\frac{\delta - k v_L}{\gamma'}\right)^2}, \qquad \gamma' = \gamma\sqrt{1+s_0}$$

is the power broadened absorption rate; $s_0 = I/I_s$ is the saturation parameter defined as the intensity of the laser beam divided by the on-resonance saturation parameter, γ the linewidth of the transition, δ the detuning of the probe laser with respect to

the transition frequency, k the wave number and v_L the velocity component in the direction of the laser beam.

If $t_a < \Delta t$, the atom will absorb a photon and its velocity and position are adapted accordingly. Next, the atom is allowed to decay spontaneously or by stimulated emission and after that the cycle starts again. The time it would take the atom to make a spontaneous or stimulated decay is calculated just as for the absorption, where for the spontaneous decay $W = \gamma$, and the process which takes the least time is chosen. These absorption-emission cycles slightly change the velocity of the atom and thus cause a difference in the absorption of the probe laser when the pump laser is on or off.

The absorption of the probe laser is simulated by the same equations as for the pump laser, but now each time an atom absorbs a photon the absorption A is increased by one. This process is repeated for several thousand atoms at each detuning, both for zero laser power of the pump laser and for power P. The resulting values $A(\nu, P)$ and $A(\nu, 0)$ are subtracted which yields the dispersive signal that can be compared to the experimental data.

4.4 Discussion

To simulate the LiPS spectra the MC calculations were performed for specific laser frequencies spanning a frequency range of 200 MHz around the resonance frequency. At each frequency 50.000 atoms were tracked. The associated statistical uncertainties are indicated in Fig. 4.9 as a band. This figure shows the results of the MC simulation for a laser power of 3 mW ($s_0 = 2.5$) in comparison to the measured LiPS signal. Considering the profile of the LiPS signal, there is clearly good agreement between the simulation and the experimental data. The MC simulation shows that mainly the positions of the maximum and the minimum and the wings of the spectrum depend on the exact shapes of the transverse velocity distributions, i.e. the widths of the distributions.

The most important feature from a frequency-locking point of view is that the zero-crossing turns out to depend barely on the width of the initial transverse velocity distribution. Also, the zero-crossing is only weakly dependent on the pump power, cf. Fig. 4.10. This makes the dispersive LiPS signal suited for laser-frequency locking. For the laser powers used ($0.75 \leq s_0 \leq 4$) the zero-crossing is slightly red-detuned by $0.1 - 0.2$ units of Γ. The MC results are in agreement with the LIF determination of the zero crossing of the LiPS signal.

The results from the Doppler-free saturation spectroscopy show a similar frequency dependence but deviate in absolute value by about 0.3 units of Γ. Just as in the present beam experiments, in Doppler-free saturation spectroscopy the pump beam modifies the velocity distribution [74–79]. Therefore the maximum in the Doppler-free saturation spectroscopy signal does not necessarily coincide with the atomic resonance frequency. Earlier studies [77–79] predict a blue shift of the maximum of the saturation absorption peak with respect to the transition in the order of 0.1 units of Γ. The remaining shift of 0.2 Γ (7 MHz) can well be explained by a small ($\sim 1°$) angular deviation of our saturation absorption beams with respect to the atomic beam. To have

the saturation absorption spectroscopy pump and probe beam overlap there is a small angle of 2° between them, which makes an accurate (< 1°) overall alignment of both beams with respect to the atomic beam difficult. Given this small angular uncertainty the saturation absorbtion spectroscopy data are consistent with the LIF data.

4.5 Conclusion

It has been shown that the absorption of a probe beam crossing an atomic beam downstream from and in opposite direction of a pump beam yields a dispersive signal. The zero-crossing of this Light Pressure induced Spectroscopy (LiPS) signal is approximately 0.1 - 0.2 line widths red-shifted from the atomic resonance frequency. The position of the zero-crossing depends only weakly on beam properties and laser power. This makes the LiPS signal very suitable for laser-frequency locking. The long term frequency fluctuations when the laser was locked to the LiPS signal were measured to be 0.12 MHz only. The exact shift of the zero-crossing is determined by laser-induced fluorescence. A Monte-Carlo description was developed to simulate the LiPS signals. Good agreement was found between the experimental data and the MC simulations.